

Analytical Assessment of Earthquake Energy Demand in Single Degree of Freedom Systems

Kimheng Oeung¹, Piseth Doung^{1,2*}, Sutat Leelataviwat³, Virak Han¹

¹ Department of Civil Engineering, Faculty of Civil Engineering, Institute of Technology of Cambodia, Russian Federation Blvd., P.O. Box 86, Phnom Penh, Cambodia.

² Materials and Structures Research Unit, Research and Innovation Center, Institute of Technology of Cambodia, Russian Federation Blvd., P.O. Box 86, Phnom Penh, Cambodia.

³ Department of Civil Engineering, Faculty of Engineering, King Mongkut's University of Technology Thonburi, 126 Pracha Uthit Rd, Bang Mot, Thung Khru, Bangkok 10140, Thailand.

Received: 11 February 2021; Accepted: 12 February 2022; Available online: June 2022

Abstract: Most seismic design methods generally use an equivalent-static lateral forces known as an elastic method to generate the lateral design force from the earthquake ground motions. Although this method is permissible under design ground acceleration, the accurate inelastic response is not well explained and still remains in extensive studies. In this regard, cumulative energy dissipation is an integral part of the design process in order to ensure that a seismic-resistant structure achieves the target structural performance. Existing studies have indicated the assessment method for the energy demand of a single degree of freedom system (SDOF) can be evaluated analytically, and the hysteretic energy can be described in relations with the system's input energy. Thus, this paper assesses the earthquake energy demand of SDOF systems using an analytical software so-called "Perform 3D". This study also aims to discuss and compare the energy demand of SDOF systems from different analytical calculations with those from Perform 3D. The study considered a SDOF system represented by a lateral cantilever column with potential plastic hinge at its fix base. The SDOF systems was numerically performed under six earthquake ground motions selected from Pacific Earthquake Engineering Research (PEER) database. All the ground motions were intensively scaled to match the two design earthquake levels, namely design basis earthquake (DBE) and maximum considered earthquake (MCE). Nonlinear time history analysis was used to evaluate the energy demand corresponding to various structural periods and ductility. Finally, the energy demand results were compared and discussed with the existing analytical calculations, as described earlier, in terms of energy factor. The numerical results showed that the energy factors ranged from 0.23 to 0.57 for a strength reduction factor of $R = 1.5$ to 3, respectively. This finding also suggested further theoretical and numerical studies on the energy factor for the development of energy-based design method.

Keywords: Input energy; Hysteretic energy; Single degree of freedom; Energy demand; Cantilever column

1. INTRODUCTION

Until recently, a direct performance-based seismic design method is favorable for extensive study. This is because the structural performance can be controlled in a direct manner. Many researches have indicated that under severe earthquakes, the structural members may undergo large inelastic deformations [1-4]. However, currently design approaches are limited to directly account for the cumulative damage effect

caused by large inelastic deformations. A structural component gradually increases more damage, then the dissipated energy capacity becomes minimal. Researchers have been put eyes at the cumulative impacts of repetitive inelastic deformations on the general structures during a severe earthquake, and then is considered as "energy-based design" [5]. The energy-based concept was first introduced by [6]. Subsequently, the direct seismic design based on energy method has been developed. The

* Corresponding author: Piseth Doung
E-mail: piseth@itc.edu.kh; Tel: +855-12 472 517

development of the energy-based method still remains a remarkable challenge due to the uncertain seismic ground motions and structural properties. Several researchers have predicted energy demand spectra, both hysteretic and input energy for a SDOF system [7-10]. The hysteretic energy can be described in relations with the input energy of the system. However, none of the other studies has shown that those significant findings are usable. Therefore, this study aimed to investigate, discuss and compare the energy demand between the analytical calculations from existing studies and the software perform 3D for the SDOF systems in order to provide a comprehensive point of view of the hysteretic energy demands. A SDOF system is represented by a mass m located at the roof level of a cantilever column.

2. Energy demand predictions

The theoretical study of the hysteretic energy design method relied on the expressions given by Dindar et al. [9] and Alici & Sucuoğlu [7]. Moreover, a software called Perform 3D was also used as a numerical study to predict the energy demand of the SDOF system. The SDOF system is represented by a lateral cantilever column with potential plastic hinging near its fix base. A wide flange shape column of W8x24 was selected for the study.

The column was modeled as bi-linear moment rotation component, considering strength degradation. The modeling method can be found in ASCE 41-17 (2017) [11]. The SDOF system was subjected to six earthquake ground motions which were scaled to design basis earthquake (DBE) and maximum-considered earthquake (MCE) levels. The variation of strength reduction factor, $R = 1.5, 2, 2.5, 3$ had been considered to ensure the validity of the results. The fundamental period of the systems was considered to be 0.5s, 0.75s, and 1.0s. The mass of the system corresponding to the fundamental period is 1410kg, 3170kg, and 5639kg, respectively. The step-by-step process is described as follows:

Step 1. Structural modeling, ground motion record, and design response spectrum with 5% damping.

Step 2. Scale the ground motions up to the earthquake hazard level with the corresponding fundamental period. Cumulative hysteretic energy was calculated based on Dindar et al. [9] and Alici and Sucuoğlu [7].

Step 3. Nonlinear time-history analyses were performed using PERFORM-3D.

Step 4. Energy terms are determined from the results of nonlinear time history analyses. This process is repeated within a range of fundamental periods and earthquake records.

Step 5. Hysteretic energy is plotted with respect to the given period range. Finally, the results of all approaches are discussed and compared.

2.1 Energy equations for single-degree-of-freedom systems

Uang and Bertero [12] first proposed direct integration

of the equation of motion concerning the relative displacement of the system can derive the energy balance equation.

$$m\ddot{u} + c\dot{u} + f_s = -m\ddot{u}_g \quad (\text{Eq. 1})$$

where:

- m = mass of the system
- c = coefficient of damping
- f_s = restoring force
- \ddot{u}_g = ground acceleration
- u = relative displacement
- \dot{u} = relative velocity
- \ddot{u} = relative acceleration

The energy equation for the SDOF system based on relative motion can be modified as

$$\int m\ddot{u}\dot{u}dt + \int c\dot{u}^2dt + \int f_s\dot{u}dt = -\int m\ddot{u}_g\dot{u}dt \quad (\text{Eq. 2})$$

where:

- $E_K = \int m\ddot{u}\dot{u}dt = \frac{1}{2}m\dot{u}^2$ = relative kinetic energy
- $E_D = \int c\dot{u}^2dt$ = damping energy
- $E_A = \int f_s\dot{u}dt$ = absorbed energy
- $E_I = -\int m\ddot{u}_g\dot{u}dt$ = relative input energy

However, the absorbed energy E_A also includes hysteretic E_H and E_S energies caused by the elastic response of the system, respectively, and it is expressed as:

$$E_A = E_S + E_H \quad (\text{Eq. 3})$$

Then the Eq. (2) can be written as

$$E_H = E_I - (E_K + E_D + E_S) \quad (\text{Eq. 4})$$

The input energy (E_I) can be divided into two categories: recoverable and dissipated energies. Within structures, elastic strain energy (E_S) and kinetic energy (E_K) are retained, and then when the vibration of the system stops, it disappears. On the other hand, the damping (E_D) and hysteretic (E_H) energies are dissipated during motion.

2.2 Input and hysteretic energies

Hysteretic energy is equal to the area of bounded hysteretic loops when the structure experiences an earthquake, as shown in Fig.1. For the single degree of freedom system as shown in Fig.2, the cumulative hysteretic energy can be estimated with the input energy.

Housner [6] first introduced the input energy equations of a SDOF system and the hysteretic energy equation was developed in relations with the input energy. Akiyama [13] had then developed an energy procedure of multi-story buildings which is equivalent to a single degree of freedom (SDOF) system. In similar year, Fajfar et al. [2] introduced an input energy formula related to the strong ground motions given by Trifunac & Brady

[14]. Then, a parametric study of SDOF systems was investigated by Fajfar & Vidic [15]. Dindar et al. [9] used six different constitutive models and 228 records to predict the seismic energy demand of the SDOF systems. The expression of input energy and hysteretic energy was derived from the energy concept, and can be seen in Eq. (5) and Eq. (7), respectively. Alici & Sucuoğlu [7] also proposed an energy spectrum method using equivalent pseudo-velocity to estimate the input energy. Five ground motions with the effect of soil type, epicentral distance, moment magnitude, and fault type on input energy had been considered.

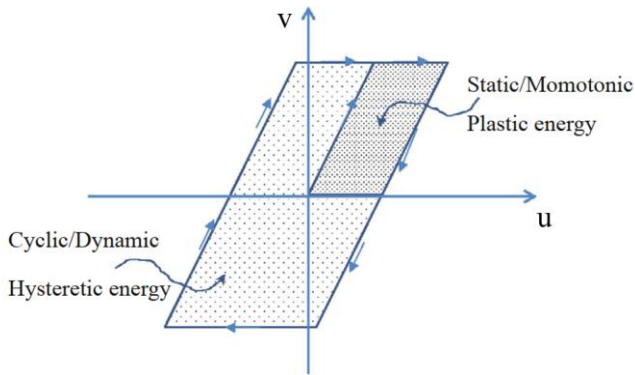


Fig. 1. Elastic perfectly plastic hysteresis loop [16]

The input and hysteretic energy based on Dindar et al. [9] can be estimated as follow:

$$E_I = (PGA/0.1g)^2 \times E_I^{0.1g} \times m \quad (\text{Eq. 5})$$

where:

PGA = peak ground acceleration

$E_I^{0.1g}$ = mass normalized input energy for the base seismic intensity (PGA = 0.1g)

The expression of $E_I^{0.1g}$ can be shown as

$$E_I^{0.1g} = \begin{cases} A + \frac{(B-A)(T-0.05)}{T_C-0.05} & 0.05s \leq T \leq T_C \\ B(T_C/T)^k & T_C \leq T \leq 3.0s \end{cases} \quad (\text{Eq. 6})$$

Where:

A, B, k and T_C = coefficient depending site class and ductility

Whereas the formulation of the cumulative hysteretic energy is the same as input energy by different parameters

$$E_H = (PGA/0.1g)^2 \times E_H^{0.1g} \times m \quad (\text{Eq. 7})$$

$$E_H^{0.1g} = \begin{cases} A + \frac{(B-A)(T-0.05)}{T_C-0.05} & 0.05s \leq T \leq T_C \\ B(T_C/T)^k & T_C \leq T \leq 3.0s \end{cases} \quad (\text{Eq. 8})$$

Based on Alici & Sucuoğlu [7], the equivalent velocity for the energy calculation can be estimated as follows

$$V_{eq} = [a \cdot e^{-bT} + c]S_v \quad (\text{Eq. 9})$$

Where:

a, b, and c = numerical factors depending on the damping and period

S_v = pseudo velocity from the elastic response spectrum

The input energy can be expressed as

$$E_I = \frac{1}{2}m[a \cdot e^{-bT} + c]^2 S_v^2 \quad (\text{Eq. 10})$$

By assuming the ratio of the cumulative hysteretic energy to the input energy to be 0.6-0.8 [10], the cumulative hysteretic energy can be computed as

$$E_H = 0.6 \frac{1}{2}m[a \cdot e^{-bT} + c]^2 S_v^2 \quad (\text{Eq. 11})$$

2.3 Modeling assumptions for the analyzed systems

Nonlinear time-history analyses were conducted. The model for this system is represented by a lumped-mass lateral cantilever column with potential plastic hinging near its fix base. The mass was adjusted corresponding to the fundamental period. The yield capacity of the column was modified to match the selected strength reduction factor, R, where $R = mS_a/V_y$; m is the mass of the system, S_a is the design spectral acceleration, and V_y is the design base shear [5].

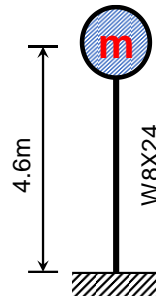


Fig. 2. Lateral cantilever column

2.4 Nonlinear time history analysis

The objective of nonlinear time history analysis is to compute the energy demand. This approach used the selected ground motions and scaling them up at a hazard level. All the ground motions were appropriately selected based on the PEER NGA database in which the record criteria are recommended. A methodology in FEMA (2009) [17] utilizes a set of far-field ground motions with three pairs of horizontal components in both directions (X and Y direction). Six ground motion were selected for this study. The selected ground motions can be seen in Table 1. The unscaled spectral acceleration is shown in Fig. 3.

All the six ground motions were scaled up to DBE and MCE hazard levels. The scaling process involves two factors, normalization, and scaling (anchoring). A ground motion was

normalized to avoid the unwarranted variability between records due to different magnitude, source distance, source type, and site conditions. The ground motion database gave the normalized factor for each ground motion. The scaling to DBE and MCE levels depended on the spectral acceleration of all ground motions. The spectral acceleration of all ground motion was scaled up to the represent DBE and MCE levels at the actual fundamental period from the analysis.

Table 1 Selected set ground motions records

ID	RS No.	Site Class	Component	Horizontals records	PGA (g)
1	953	D	1	NORTHR/MUL009	0.44
2			NORTHR/MUL279	0.49	
3	960	D	1	NORTHR/LOS000	0.40
4			NORTHR/LOS270	0.47	
5	1602	D	1	DUZCE/BOL000	0.74
6			DUZCE/BOL090	0.81	

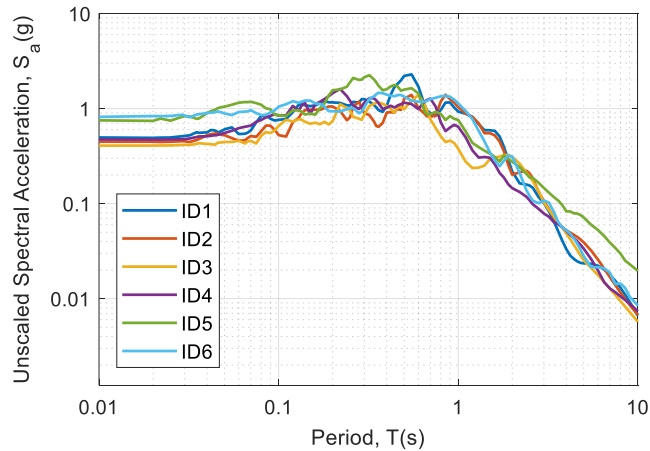


Fig. 3. Unscaled spectral acceleration of the six records

3. RESULTS AND DISCUSSION

3.1 Design response spectrum

Soil site condition was taken from a previous study by Doung [18]. The structural system was assumed to be a Design Category D with $S_1 = 0.6g$ and $S_s = 1.5g$ [19]. For a reason of insufficient seismic data in Cambodia, soil class D was chosen. The soil condition is similar to the soil located at San Francisco. The study was evaluated at two hazard levels, DBE and MCE. The design spectral acceleration values were determined and are shown in Fig. 4 and Table 2 below.

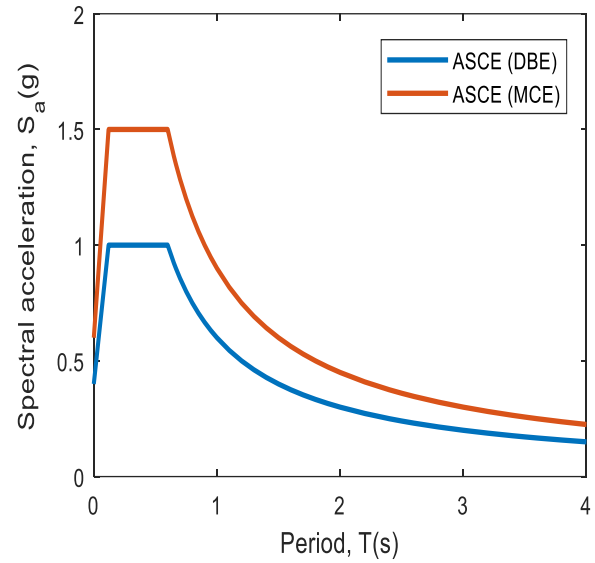


Fig. 4. Design response spectrum for DBE and MCE level

Table 2 Design spectral acceleration of the SDOF system

Period T (s)	DBE	MCE
0.50	1.00	1.50
0.75	0.80	1.20
1.00	0.60	0.90

3.2 Energy Demands in Single Degree of Freedom Systems

The comparison was assessed between Dindar, Alici, and Perform 3D. As shown in Figs. 5 and 6, the input energy from Dindar increased linearly from period 0.05s until it reached a peak at $T = 0.75s$. Then there was a steady deterioration until $T = 3.0s$. The input energy from Dindar did not significantly change in accordance with different reduction factors (R).

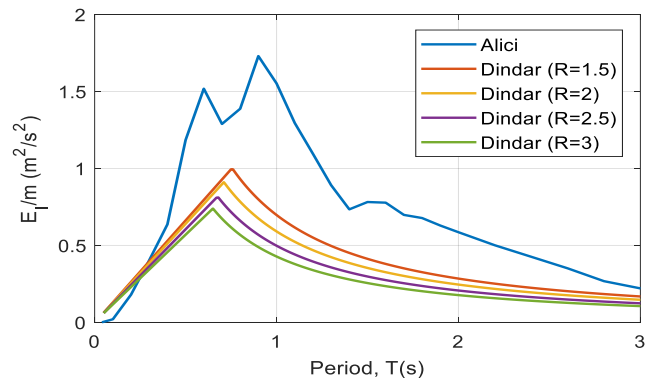


Fig. 5. Input energy for SDOF for DBE level ($S_a = 1g$)

It is worth noting that Dindar delivered a calculation procedure with a standard shape of the input energy. Alici also provided a similar pattern to Dindar which a peak point is at a period of approximately 0.9s.

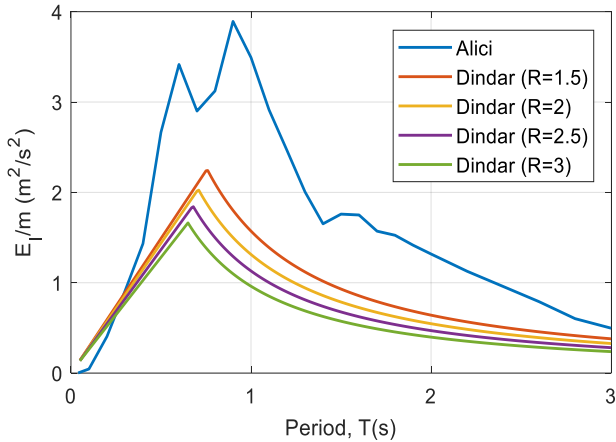


Fig. 6. Input energy for SDOF for MCE level ($S_a = 1.5g$)

and input energy provided similar manner in the amount of energy difference.

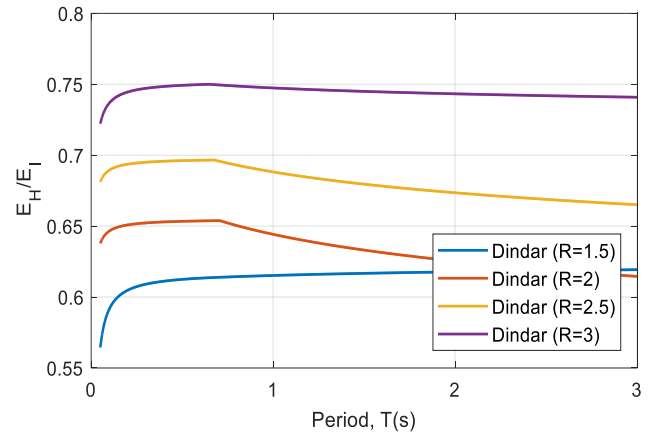


Fig. 8. Ratio of hysteretic to input energy for MCE level ($S_a = 1.5g$)

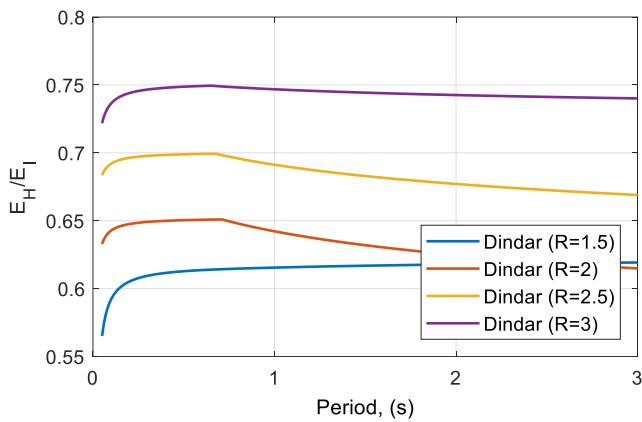


Fig. 7. Ratio of hysteretic to input energy for DBE level ($S_a = 1.5g$)

An energy ratio is defined as the ratio between hysteretic energy and input energy, E_H/E_I . For both DBE and MCE hazard levels, the E_H/E_I ratio was found to range from 0.6 to 0.8, as shown in Figs.7 and 8. As can be seen, by the strength reduction factor, R , the level of plasticity does not significantly influence the hysteretic energy demands. Thus, the energy factor E_H/E_I for the system can be considered to be from 0.6 to 0.8. This observation was similar to a recommendation given by Fajfar et al. [10].

The total input energy obtained from Perform 3D was then delivered for the discussion and comparison. Figs 9 and 10 describes the total input energy for DBE and MCE hazard levels, respectively. Figs 11 and 12 show the total hysteretic energy. As can be seen, the charts showed that both hysteretic energy

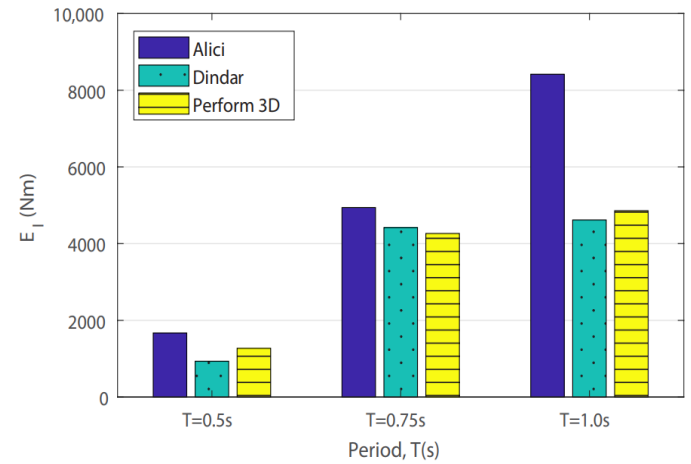


Fig. 9. Comparison of input energy for SDOF for DBE level ($R=1.5$)

As observed earlier, the maximum input energy from Dindar et al. [9] became maximum at a period of approximately 0.75s. However, the total input energy from Alici & Sucuoğlu [7] rose sharply depending on the mass of the system. Therefore, the total input energy from Dindar et al. [9] is similar to Perform 3D rather than Alici & Sucuoğlu [7].

The result from Perform 3D of the energy factor (E_H/E_I) depended on the strength reduction factor R is shown Figs. 13 and 14, respectively. As seen, the energy ratio (E_H/E_I) increased when the strength reduction factor (R) was increased. Meanwhile, when $R = 1.5$, the ratio E_H/E_I is approximately 0.25. However, the energy ratio increased to around 0.6 when $R = 3$. This finding agreed with the result from Dindar et al. [9] in the previous discussion that the energy ratio E_H/E_I ranged from 0.6 to 0.8.

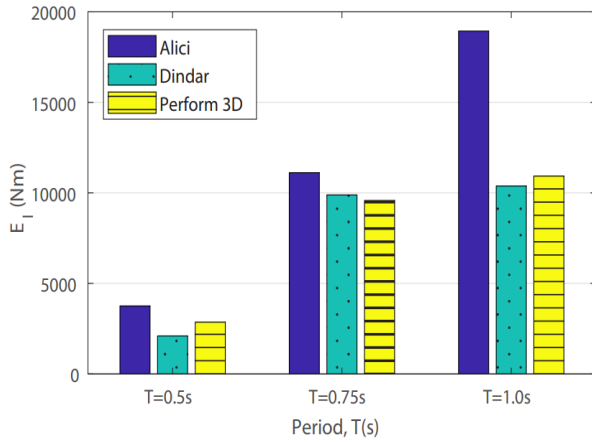


Fig. 10. Comparison of input energy for SDOF for MCE level (R=1.5)

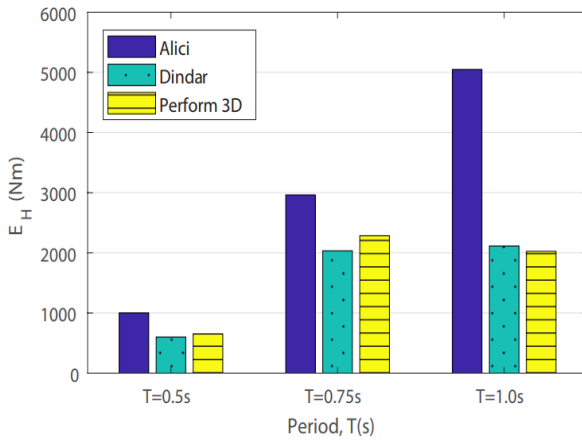


Fig. 11. Comparison of hysteretic energy for SDOF for DBE level (R=3)

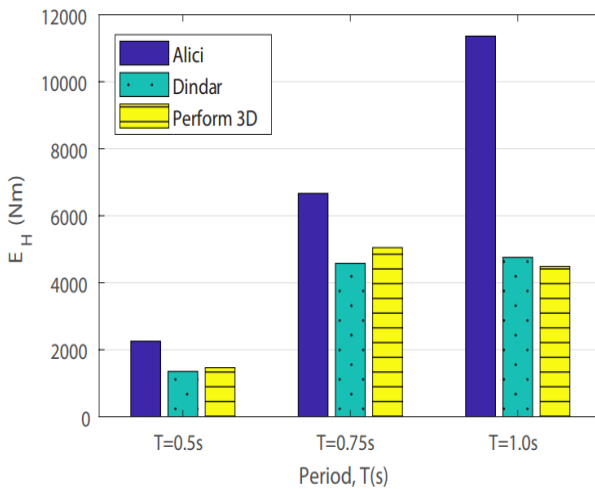


Fig. 12. Comparison of hysteretic energy for SDOF for MCE level (R=3)

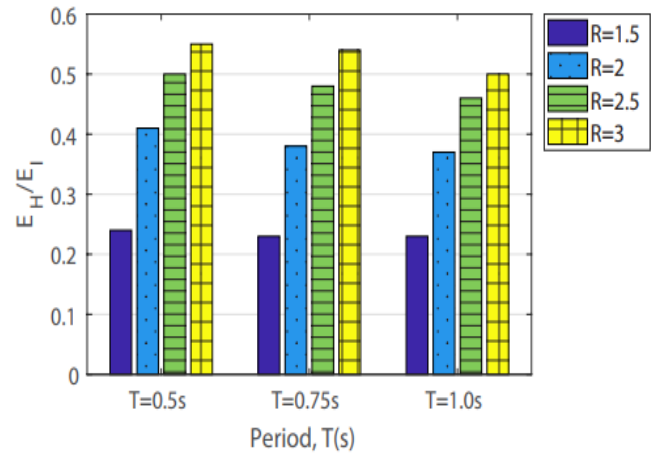


Fig. 13. Modification factor (γ or E_H/E_I) at DBE level from Perform 3D

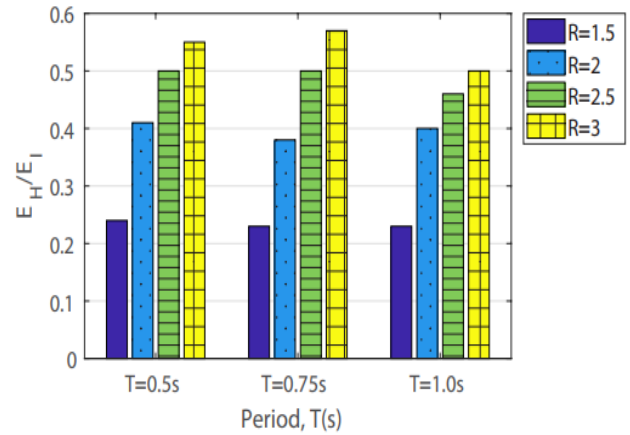


Fig. 14. Modification factor (γ or E_H/E_I) at MCE level from Perform 3D

4. CONCLUSIONS

This investigation discussed and compared the energy demands between the analytical calculation from existing studies and those from a software called Perform 3D. The application of the energy calculation was presented. Based on the results, the following conclusions can be drawn:

- The energy factor (γ) depended on the strength reduction factor (R), ductility factor (μ), and fundamental period (T) for the system ($R - \mu - T$). The value of γ increased when R and μ increased. However, the relations between γ and T were not put into attention. Further study should include this consideration, including effect of soil types.
- The energy factor from Dindar et al. [9] provided a value of approximately 0.6, almost similar to an assumed value given by Fajfar et al. [10]. However, the energy factor from

Perform 3D ranged from 0.23 to 0.57. As for manual calculation, the modification factor from Perform 3D can be chosen to the upper bound value of about 0.6, which is the same as Dindar et al. [9] and Fajfar et al. [10], and rational for seismic application.

This study provides the first comprehensive picture of the hysteretic energy demands. However, it has limitations in terms of the structural types and model accuracy. Further research is needed to clearly understand the fundamentals of energy demand, including the energy modification factor.

ACKNOWLEDGMENTS

Authors wish to thank King Mongkut's University of Technology Thonburi (KMUTT) in Thailand for financial support on this research project..

REFERENCES

- [1] Chao, S.-H., Goel, S. C., & Lee, S.-S. (2007). A Seismic design lateral force distribution based on inelastic state of structures. *Earthquake Spectra*, 23(3), 547–569. <https://doi.org/10.1193/1.2753549>
- [2] Fajfar, P., Vidic, T., & Fischinger, M. (1989). Seismic demand in medium- and long-period structures. *Earthquake Engineering & Structural Dynamics*, 18(8), 1133–1144. <https://doi.org/10.1002/eqe.4290180805>
- [3] Lee, S.-S., & Goel, S. C. (2001). Performance-Based Design of Steel Moment Frames Using Target Drift and Yield Mechanism. PhD Thesis, University of Michigan, Ann Arbor, Michigan.
- [4] Leelataviwat, S., Goel, S. C., & Stojadinović, B. (1999). Toward performance-based seismic design of structures. *Earthquake Spectra*, 15(3), 435–461.
- [5] Erduran, E. (2020). Hysteretic energy demands in multi-degree-of-freedom systems subjected to earthquakes. *Buildings*, 10(12), 220. <https://doi.org/10.3390/buildings10120220>
- [6] Housner, G. W. (1956). Limit design of structures to resist earthquakes, in *Proceedings of the 1st World Conference on Earthquake Engineering*, vol. 5, pp. 1-13, Berkeley, Calif, USA, June 1956.
- [7] Ahcı, F. S., & Sucuoğlu, H. (2016). Prediction of input energy spectrum: attenuation models and velocity spectrum scaling: input Energy Spectrum. *Earthquake Engineering & Structural Dynamics*, 45(13), 2137–2161. <https://doi.org/10.1002/eqe.2749>
- [8] Decanini, L. D., & Mollaioli, F. (1998). Formulation of elastic earthquake input energy spectra.
- [9] Dindar, A. A., Yalçın, C., Yüksel, E., Özkaynak, H., & Büyüköztürk, O. (2015). Development of earthquake energy demand spectra. *Earthquake Spectra*, 31(3), 1667–1689. <https://doi.org/10.1193/011212EQS010M>
- [10] Fajfar, P., Vidic, T., & Fischinger, M. (1992). On energy demand and supply in SDOF systems. *Nonlinear Seismic Analysis and Design of Reinforced Concrete Buildings*, 41–62.
- [11] ASCE 41-17. (2017). *Seismic Evaluation and Retrofit of Existing Buildings*. American Society of Civil Engineers, Reston, Virginia. <https://doi.org/10.1061/9780784414859>
- [12] Uang, C.-M., & Bertero, V. V. (1990). Evaluation of seismic energy in structures. *Earthquake Engineering & Structural Dynamics*, 19(1), 77–90. <https://doi.org/10.1002/eqe.4290190108>
- [13] Akiyama, H. (1985). *Earthquake-resistant limit-state design for buildings*. University of Tokyo press, Tokyo.
- [14] Trifunac, M. D., & Brady, A. G. (1975). A study on the duration of strong earthquake ground motion. *Bulletin of the Seismological Society of America*, 65(3), 581–626.
- [15] Fajfar, P., & Vidic, T. (1994). Consistent inelastic design spectra: Hysteretic and input energy. *Earthquake Engineering & Structural Dynamics*, 23(5), 523–537. <https://doi.org/10.1002/eqe.4290230505>
- [16] Mezgebo, M. G., & Lui, E. M. (2017). A new methodology for energy-based seismic design of steel moment frames. *Earthquake Engineering and Engineering Vibration*, 16(1), 131–152. <https://doi.org/10.1007/s11803-017-0373-1>
- [17] FEMA. (2009). *Recommended Methodology for Quantification of Building system Performance and Response Parameters*.
- [18] Doung, M. P. (2016). *Seismic Collapse Evaluation of Buckling-Restrained Knee-Braced Frames with Single Plate Shear Connections*. Master Thesis, King Mongkut's University of Technology Thonburi, Bangkok, Thailand
- [19] ASCE 7-10 (2010). *Minimum Design Loads for Buildings and Other Structures*. American Society of Civil Engineers, Reston, Virgin